T E C H N I C A L
R E P O R T

0653

MIXTURE DISTRIBUTIONS TO MODEL DATA FROM IN VITRO-IN VIVO CORRELATION EXPERIMENTS

JACOBS, T., ROSSENU, S., DUNNE, A., MOLENBERGHS, G., STRAETEMANS R.

and L. BIJNENS

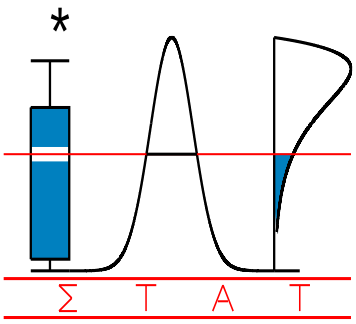

I A P S T A T I S T I C S
N E T W O R K

INTERUNIVERSITY ATTRACTION POLE

http://www.stat.ucl.ac.be/IAP

Mixture Distributions to Model Data From *In Vitro-In Vivo Correlation* Experiments

Tom Jacobs[1], Stefaan Rossenu[3], Adrian Dunne[2], Geert Molenberghs[1], Roel Straetemans[3], Luc Bijnens[3]

[1]Hasselt University, Center for Statistics, Agoralaan 1, B-3590 Diepenbeek, Belgium

[2]UCD School of Mathematical Sciences, University College Dublin, Belfield, Dublin 4, Ireland

[3]Johnson and Johnson Pharmaceutical Research and Development,

a division of Janssen Pharmaceutica N. V. Turnhoutseweg 30, B-2340 Beerse, Belgium

Summary

A method is presented to describe the *in vitro-in vivo correlation* of an extended release drug formulation. This extended release drug product is overencapsulated with immediate release material. The heterogeneity of the capsule is modelled using a mixture distribution of an extended release and an immediate release pharmacokinetic profile. Whereas an IVIVC is conventionally performed using a two-stage procedure, the model of this mixture uses the convolution-based method with a one-stage approach. The method is applied to a Galantamine controlled release formulation, an acetylcholinesterase inhibitor for the treatment of Alzheimer's disease. The average percentage prediction error indicated a good fit of the new model using the logit link function.

Keywords: controlled release; convolution; dissolution curve; IVIVC; one-stage model fitting.

1 Introduction

In Vitro-In Vivo Correlation (IVIVC) is commonly used in preclinical and clinical biopharmaceutical research. It establishes a valuable link between the *in-vitro* dissolution and the

in-vivo release of the investigational drug. Based on this link, the controlled release pharmacokinetic profile can be predicted from a subject's immediate release plasma concentrations profile and the *in-vitro* dissolution profile using the IVIVC model. If a controlled release capsule dissolves differently, this change in *in-vitro* dissolution properties can be translated into the corresponding altered *in-vivo* pharmacokinetic profile once an IVIVC is established.

IVIVC models are commonly used in a wide range of applications. One can use the IVIVC to claim that the differences observed *in-vitro* between two batches do not affect the drug exposure by predicting the *in-vivo* plasma concentration-time profile. Similarly, one can state that manufacturing changes of the controlled release formulations do not affect the drug exposure. Thus no expensive *in-vivo* bioequivalence testing is required for either situation (Hayes 2004). This technique can also be applied in formulation development. The formulation can be modified such that the plasma concentrations remain within the therapeutic window over a sufficient period of time.

The first methodological work on IVIVC was done two decades ago (Gillespie *et al.* 1985) with the introduction of the deconvolution method: deconvolution extracts the *in-vivo* release based on the fact that controlled release plasma concentrations equal the convolution of immediate release plasma concentrations and the *in-vivo* release. The latter is then linked to the *in-vitro* dissolution results. Dunne *et al.* (2005), however, proved that the deconvolution method might give biased results. Gillespie (1997) and O'Hara *et al.* (2001) improved the method by directly modelling the convolution itself, without explicitly calculating the *in-vivo* release, using a two-stage approach.

Our methodology presented in this paper also uses the convolution approach and extends previous work in two respects. The two-stage approach is replaced by a one-stage approach and contrary to other published results (Modi *et al.* 2000, Veng-Pedersen *et al.* 2000) a heterogeneous formulation is used in the IVIVC model. The formulation contains an extended release part overencapsulated with immediate release material, and will be referred to as controlled release capsule in the remainder of the paper.

The rest of the paper is organized as follows. The case study, motivating this research,

is described in Section 2. The convolution-based models described by O'Hara *et al.* (2001) used for IVIVC can be found in Section 3.2.1. The dissolution models applied in this paper are described in Section 3.1. Extension of these models including a mixture distribution is described in Section 3.2.2. The results of applying the proposed methodology to the case study are reported in Section 4.

2 The Case Study

The acetylcholinesterase inhibitor Galantamine is used for the treatment of Alzheimer's disease (Lilienfeld 2002). Galantamine formulations currently on the market are tablets, a syrup and extended-release capsules.

Within the population of subjects with Alzheimer's disease, the duration of drug exposure can sometimes be too short to guarantee sufficient protection for a certain time period due to poor compliance. Therefore, a controlled release formulation of Galantamine was developed in an attempt to optimize drug exposure. Whereas an immediate release formulation dissolves instantaneously and the drug product is immediately available, an extended release formulation releases the drug product slowly over time allowing the body to absorb the drug product gradually. The controlled release formulation under investigation here consisted of the extended and immediate release components combined in the same pellet as 2 layers (ratio CR/IR: 3/1) separated by a rate-controlling membrane containing 5-12% ethylcellulose/hydroxypropyl-methylcellulose (EC/HPMC; ratio: 75/25). The relatively high water solubility (3.3 g/100 $m\ell$ water, pH=5.2) and absolute oral bioavailability (88.5%) of Galantamine are pharmaceutical characteristics indicative of a drug whose controlled release formulation is a good candidate for IVIVC exploration.

For each controlled release formulation, twelve dissolution curves were assessed *in-vitro*. The dissolution data were generated using an USP apparatus 2 - paddle with 50 rpm (s.e. 2 rpm) speed of shaft rotation. The dissolution medium used was a volume of 900 $m\ell$ of 0.050 M phosphate buffer at pH 6.5. The percentage dissolution was registered between 0.5 and 18 hours, as shown in Figure 1 for the controlled release formulation.

Seventeen subjects were first assigned to the immediate release formulation and then randomized according to a four period latin square design. Treatments were four controlled release formulations (slow, fast, between and medium) of Galantamine. One subject dropped out after the immediate release period. He did not receive the controlled release formulations and was included as such in the analysis. To demonstrate our methodology, only one of the four controlled release formulation, the slow one, is included in this analysis. A venous blood sample was taken for the measurement of Galantamine plasma concentrations at specified time points during the study, from pre-dose (0 hour) until 60 hours post-dose for the immediate release formulation, and up to 72 hours post-dose for the controlled release formulations.

The immediate release plasma concentration-time data are shown in Figure 2, while the plasma concentration-time data for the controlled release formulation are presented in Figure 3. In the former, maximal plasma concentrations were reached faster and were higher, but they decreased rapidly. In the latter, a bimodal profile was present: one steep peak was present after 30 minutes followed by a second smoother peak 6 hours after intake. In addition, the decrease of plasma concentration is slower after the second peak.

The advantage of combining the extended and immediate release formulation lies in this bimodal profile. The extended release part ensures that patients remain in the effective plasma concentration range from 3-4 until 24 hours. The extended release fraction on it own would not reach the therapeutic window quickly enough; levels would remain too low during the first 3 hours post-dose. Therefore, a loading dose consisting of an immediate release fraction, is added. Hence, patients remain protected for the full 24 hours.

3 Methodology

First, three types of models used for describing the *in-vitro* dissolution curves are introduced in Section 3.1. Then the *in-vivo* convolution-based IVIVC methodology described by O'Hara *et al.* (2001) is described in Section 3.2.1, followed by the newly proposed convolution model in Section 3.2.2, the model fitting in Section 3.3 and the goodness-of-fit in Section 3.4.

The following notation will be used. The index 1 denotes the *in-vitro* data, while 2 will be used for *in-vivo*, i is the statistical unit representing the capsule for *in-vitro* and subject for the *in-vivo* data; k denotes the formulation; The immediate release formulation however will be denoted with δ instead of k due to its special status in IVIVC modelling and to emphasize that the underlying probability density function of the release mechanism follows in this case the Dirac Delta distribution. F will denote the actual dissolution/release fraction; c stands for the actual plasma concentration profile, and more specific, $c_{i2\delta}$ is the actual immediate release plasma concentration profile, also referred to as the unit impulse response. This is traditionally but not necessarily, based on a compartmental model. Y_1 stands for the measured dissolution for the *in-vitro* data, Y_2 for measured plasma concentration *in-vivo*. For example, Y_{i2k} denotes the measured controlled release plasma concentration of subject i for formulation k.

3.1 *In-Vitro* Dissolution Models

The *in-vitro* dissolution profile is often described by a Weibull function (Comets and Mentré, 2001). Besides the Weibull function, also a simpler exponential function and a more complex Gompertz *in-vitro* dissolution model will be evaluated.

The simplest model for the *in-vitro* dissolution profile is given by the exponential model:

$$\begin{aligned} Y_{i1k}(t) &= F_{i1k}(t) + \varepsilon_1, \quad \varepsilon_1 \sim N(0, \sigma_1^2), \\ F_{i1k}(t) &= \phi_1\{1 - \exp[-(t - \phi_3)\phi_{2i}]\}, \end{aligned} \tag{3.1}$$

with $\phi_{2i} \sim N(\phi_2, \sigma_{\phi_2}^2)$, and ϕ_{2i} the capsule-specific half-life and ϕ_3 a lag time. This model has a steep increase in the beginning and converges slowly to the asymptotic maximal dissolution, ϕ_1.

The following extension of the exponential model copes with the heterogeneity of the

formulation via the ϕ_5-parameter.

$$\begin{aligned} Y_{i1k}(t) &= F_{i1k}(t) + \varepsilon_1, \quad \varepsilon_1 \sim N(0, \sigma_1^2), \\ F_{i1k}(t) &= \phi_5 + (\phi_1 - \phi_5)\{1 - \exp[-(t - \phi_3)\phi_{2i}]\}, \end{aligned} \tag{3.2}$$

where ϕ_5 captures an initial jump followed by the previous version of the exponential model.

The previous models, however, lack the capability to fit a sigmoidal curvature. Therefore, the traditional Weibull function with the initial jump ϕ_5 is proposed to check for the improvement under these conditions, see model 3.3. The parameters have the same interpretation as for the exponential model.

$$\begin{aligned} Y_{i1k}(t) &= F_{i1k}(t) + \varepsilon_1, \quad \varepsilon_1 \sim N(0, \sigma_1^2), \\ F_{i1k}(t) &= \phi_5 + (\phi_1 - \phi_5)\{1 - \exp[-(\frac{t}{\phi_3})^{\phi_{2i}}]\}. \end{aligned} \tag{3.3}$$

The dissolution profiles in Figure 1 contain both an asymmetrical S-shaped curvature and an initial jump. The Gompertz curve has the first property, but it has its short curvature at the end. The following modification of the Gompertz function (Lindsey 1997) will serve to model this feature and to challenge the performance of the Weibull model:

$$\begin{aligned} Y_{i1k}(t) &= F_{i1k}(t) + \varepsilon_1, \quad \varepsilon_1 \sim N(0, \sigma_1^2) \\ F_{i1k}(t) &= \phi_5 + [\phi_{1i} - \phi_5] \exp\{-\exp[\phi_3(\phi_{2i} - t)]\}, \end{aligned} \tag{3.4}$$

where ϕ_5 represents the initial jump. The coefficient $\phi_1 \sim N(0, \sigma_{\phi_1}^2)$ corresponds to the asymptotic maximum dissolution. ϕ_{2i} represents a capsule specific lag-time, ϕ_3 corresponds to the half-life of the curve.

3.2 *In-Vivo* Models

3.2.1 Convolution-based Models (O'Hara 2001)

Gillespie (1985), Gillespie *et al.* (1997), Dunne *et al.* (1999), O'Hara *et al.* (2001), and Hayes *et al.* (2004) showed, based on *in-vitro* dissolution data and *in-vivo* immediate release

plasma concentrations, that the slow release formulation concentrations can be predicted and an IVIVC established using a convolution-based method. This method is more robust than the deconvolution method (Dunne *et al.* 2005), and it jointly fits a set of models.

The controlled release plasma concentrations at time t, denoted by $Y_{i2k}(t)$, for the ith subject taking treatment k, can be derived as the convolution of the unit impulse response $c_{i2\delta}$ and the *in-vivo* release curve F_{i2k} (Gillespie 1985):

$$\begin{aligned} Y_{i2k}(t) &= \int_0^t c_{i2\delta}(t-\tau)F'_{i2k}(\tau)d\tau + \varepsilon_2, \\ \varepsilon_2 &\sim N(0, \sigma_2^2). \end{aligned}$$

The *in-vivo* release curve F_{i2k} can be considered as the cumulative distribution function of the stochastic process representing the release of the molecule into solution. Hence, F'_{i2k} represents the corresponding density function of the release of the molecule into solution. The unobserved *in-vivo* release cumulative distribution function can be linked to the *in-vitro* one using the following IVIVC model:

$$\begin{aligned} F_{i2k}(t) &= g^{-1}(\theta_0 + \theta_1 t + s_{ik} + g(F_{1k}(t))), \\ s_{ik} &\sim N(0, \sigma_s^2). \end{aligned}$$

The parameters θ_0 and θ_1 cope with dissolution changes in the gastrointestinal tract, whereas the random effect s_{ik} represents inter-subject differences of the intestines. The link function $g(\cdot)$ can be set equal to, for example, the logit, log-log, or the complementary log-log link functions. In this paper, the link function will be limited to the logit function.

The method of O'Hara (O'Hara *et al.* 2001, Hayes *et al.* 2004) first estimates the subject-specific parameters of the immediate release profile using a compartmental analysis and in a second stage simultaneously models the *in-vitro* dissolution curves as well as the convolution using the empirical Bayes estimates from the first stage.

3.2.2 Mixture Distribution Models

All published models are limited to homogeneous formulations. A naive approach would be to ignore the heterogeneity of the formulation and fit the traditional model mentioned

above for a homogenous formulation. However, in case of a heterogenous formulation of both immediate and extended release material, the cumulative distribution function does not start at 0 but rather at a quantity approximately similar to the proportion of immediate release material within the mixture. The inclusion of this initial jump alters the density function $F'_{i2k}(\tau)$. Therefore, we propose in this section a new model that takes this heterogeneity into account.

For the convolution model a similar derivation is possible. Recall from Section 2 that the capsules represent a heterogeneous formulation, consisting in part of immediate release and in part of extended release. As a result, two different underlying dissolution processes can be expected to be present.

The principle of superposition within pharmacokinetics, i.e., the assumption that each mechanism acts independently of each other and there is linear kinetics, means that the PK concentration-time profile of the controlled release formulation can be described as a weighted combination of each of the drug product PK-concentration-time profiles. This is a valid assumption (Piotrovsky *et al.* 2003). Based on this principle, one part of the profile corresponds to the immediate release drug product within the formulation, the other one corresponds to the extended release drug product. The PK-profile corresponding to the immediate release drug product can be considered as identical to the one observed whereas the latter follows the convolution model as described in Section 3.2.1. Therefore, the following new model is proposed:

$$\begin{aligned} Y_{i2k}(t) &= \phi_5 D c_{i2\delta}(t) + [\phi_1 - \phi_5]\, D \int_0^t c_{i2\delta}(t-\tau) F'_{i2k}(\tau) d\tau + \varepsilon_2, \\ \varepsilon_2 &\sim N(0, \sigma_2^2), \end{aligned} \tag{3.5}$$

where ϕ_5 is the weight corresponding to the quantity of immediate release drug product within the formulation and D represents the dose. This corresponds to the initial jump observed in the *in-vitro* models.

Furthermore, the *in-vivo* release $F_{i2k}(t)$ model is slightly modified compared to the

proposal of O'Hara (2001):

$$F_{i2k}(t) \quad = \quad g^{-1}(\theta_0 + \theta_1 t + g(F_{i1k}(t))), \tag{3.6}$$

where the index i stands for the capsule i dependent variability of the *in-vitro* dissolution F_{i1k}. As this is unobserved for the capsule administered to the subject i, this is indirectly included via the subject level. Thus, the random effects are included at the *in-vitro* level of the model rather than as a random intercept. This corresponds to the underlying source of variation. Further, the gastro-intestinal subject level s_{ik} was removed from the IVIVC.

This newly proposed model represents a mixture distribution at two levels. A first mixture is situated in the *in-vitro* dissolution: it represents a mixture cumulative distribution function of a step function for the immediate release material of the formulation on one hand and a second cumulative distribution function such as the weibull distribution for the slow release product on the other hand. The mixture is also present at a second level: it is a combination of two normally distributed processes for the immediate release plasma concentration time-profile on one hand and the convolution based profile for the slow release product on the other hand. Again, the weight ϕ_5 comes in to attribute the ratio of the two distinct underlying release processes.

3.3 Model Fitting

The models for the immediate release plasma levels and the *in-vitro* dissolution were initially fitted separately to obtain good starting values for fitting the IVIVC model. The immediate release pharmacokinetics of Galantamine are known to follow a two-compartmental model (Piotrovsky *et al.* 2003). This was based on population modelling of several studies in elderly

patients:

$$
\begin{aligned}
Y_{i2\delta}(t) &= c_{i2\delta}(t) + \varepsilon_{i\delta k}, \\
c_{i2\delta}(t) &= \frac{k_a}{V_F}\left(\frac{(k_{21}-\alpha_i)e^{-\alpha_i(t-t_{lag})}}{(k_a-\alpha_i)(\beta_i-\alpha_i)} + \frac{(k_{21}-\beta_i)e^{-\beta_i(t-t_{lag})}}{(k_a-\beta_i)(\alpha_i-\beta_i)}\right. \\
&\quad \left. + \frac{(k_{21}-k_a)e^{-k_a(t-t_{lag})}}{(\alpha_i-k_a)(\beta_i-k_a)}\right), \\
\varepsilon_{i\delta k} &\sim N(0,\sigma_\delta^2), \qquad (3.7) \\
\begin{bmatrix} \alpha_i \\ \beta_i \end{bmatrix} &\sim N\left(\begin{bmatrix} \alpha \\ \beta \end{bmatrix}, \begin{bmatrix} s_\alpha^2 & c_{\alpha\beta}s_\alpha s_\beta \\ c_{\alpha\beta}s_\alpha s_\beta & s_\beta^2 \end{bmatrix}\right).
\end{aligned}
$$

In this model, V_F is the apparent volume of distribution, t_{lag} is a lag-time, k_a is the absorption coefficient, k_{21} the inter-compartmental clearance and α and β are clearance parameters. The best fit to the data was attained by choosing random effects on α and β, with associated variabilities σ_α^2 and σ_β^2. This was based on visual inspection of the fit of the individual profiles as well as by comparison of the likelihood functions. The absorption rate constant k_a could not be estimated by fitting the immediate release formulation alone because too few samples were taken during the absorption phase shortly after drug intake and k_a had to be fixed in the immediate release model.

A fundamental change to the convolution method of O'Hara (O'Hara *et al.* 2001) is that all models are fitted simultaneously, whereas O'Hara's method first fits the immediate release profile per subject and then in a second stage fits the convolution and the IVIVC using the empirical Bayes estimates of the immediate release PK-profile. A possible drawback of such a two-stage modelling approach is that this might lead to biased results (Verbeke and Molenberghs 2000). By using a one-stage model, this source of possible bias is eliminated. The possible impact is discussed further in Section 5.

Traditionally in pharmacokinetic modelling, the model fit is verified at the individual subject level, i.e., the question is asked whether the model can fit each subject's plasma concentration profile. Thus a hierarchical model is used. In IVIVC modelling, one is not interested in the behavior of the individual capsules or subjects, but rather in the formulation itself, at the population level. In particular, the link between the *in-vitro* dissolution and

in-vivo release process of the formulation is very important. Unlike in the linear setting, the marginal and hierarchical models do not coincide when the random effects are significant. Therefore, the random effects have to be integrated out to obtain the marginalized model. The marginalization of the hierarchical model was performed as follows: 10000 capsules were simulated and then averaged over. As such, the random effects were integrated out (Molenberghs and Verbeke 2005) and the model plotted.

The set of models was implemented in the SAS procedure NLMIXED (version 9.1). Model convergence was obtained using the first-order integration method of Beal and Sheiner (1982). The convolution integral itself was approximated with the trapezoid rule. An example of the SAS code can be found in the appendix.

3.4 Goodness-of-Fit

Following the regulatory guidances (FIP 1996, CDER 1997) the adequacy of the proposed models was assessed using the average absolute percent prediction error ($\%PE$). This was defined as the mean of

$$\left| \frac{x_{obs,i} - x_{pred,i}}{x_{obs,i}} \right| \times 100, \tag{3.8}$$

where $x_{.,i}$ is the Area Under the Curve to the last measurable observation (AUC_{last}) or the maximal concentration (C_{max}) of the empirical Bayes estimates and the observed concentrations for subject i. Thus, for each observed and predicted profile per subject, the AUC_{last} and C_{max} were calculated and the above ratios were obtained. Given its skewed distribution, all ratios were log-transformed to better approximate normality, the mean and its 90% confidence interval was calculated and backtransformed.

4 Results

As mentioned in Section 3.1, the modified Gompertz function fitted the data well. Random effects were added to ϕ_1 and ϕ_2 since, as seen in Figure 1, the asymptotic maximum dissolution was capsule dependent. The random effect on the lag time improved the fit

further.

A system of sub-models is proposed for the IVIVC modelling consisting of the combining models 3.4, 3.5, 3.6, and 3.7. All four models are fitted simultaneously. This allows exchange of information between models. Whereas the absorption rate constant k_a could not be estimated for the immediate release model alone due to insufficient early sampling points, the pooling of information about common parameters from different data sources, did allow for estimation of k_a, i.e., k_a is also present in the slow release formulation. Some simplifications were done for the system of sub-models compared to the separate models: (i) No random effect was used on the α-component of the two-compartmental model because inclusion of this random effect made the model diverge; (ii) The dissolution random effects ϕ_{i1} and ϕ_{i4} were forced to be independent otherwise estimation of the correlation could not be established.

The following models were fitted: Model (1)–(2) using the exponential dissolution and logit link without and with mixture, Model (3) with a Weibull dissolution and logit link function, and Model (4) with Gompertz dissolution and logit link. Model (2)–(4) are the newly proposed models to cope with the heterogeneity of the data. Estimates of the model parameters can be found in Table 1 for the four different dissolution curves. For comparison purposes, Table 2 was included with the parameter estimates of the Gompertz odds model and the estimates after recalculation obtained from a population modelling (Piotrovsky *et al.*, 2003) of several studies in elderly patients. V_f represents 1000 liters instead of liters as traditionally would be used. The PK-parameters obtained were within the same range as the ones obtained from the population modelling, even though k_{21} and β were estimated a factor three too high.

The fit based on the different dissolution models was not formally compared. A formal comparison would require the calculation of the Extended Information Criterion (Yafune *et al.*, 2005). Given the long time needed to fit the models, this bootstrapping procedure was considered practically infeasible. The model prediction of the controlled release plasma concentration of a randomly chosen subject for the different models is depicted in Figure 4.

The fit of the controlled release plasma concentrations was judged based on visual inspection of the empirical Bayes estimates versus the observed controlled release profiles on the one hand (Figure 5) and the average absolute percent prediction error on the other hand. The fit of the immediate release concentrations can be found in Figure 6, the fit of the *in-vitro* dissolution is presented in Figure 7 for the Gompertz odds model.

The $\%PE$ of the different models can be found in Table 3. The first two columns correspond to the C_{max} and AUC_{last} as requested in the regulatory guidelines (FIP 1996, CDER 1997), the last represents AUC_{0-4} and is an indication of the model fit for the data up to 4 hours. The model with the exponential dissolution does not fit the data well for the early time points. The addition of the mixture to the exponential dissolution improves the model. The *in-vitro* exponential mixture dissolution model however misses the S-shape as observed in the data, see Figure 7. Therefore, the model is extended to the Weibull, but the improvement was limited, and the Gompertz model with mixture distribution. This model remains under the 10% with its upper limit of the confidence interval.

In the above, the focus was on the subject level, i.e., the hierarchical model. For the correlation between the *in-vivo* and the *in-vitro* dissolution curves, one is only interested in the estimates for the formulation, not specifically at the subject level. The marginalized model, i.e., after integrating out the random effects, is visualized in Figure 8 and Figure 9.

5 Discussion

A model with clear improvements over the standard IVIVC models at two levels is presented: It allows the fitting of formulations containing both extended and immediate release material and it is a true one-stage analysis method. We employed the SAS procedure Nlmixed rather than the standardly used NONMEM package.

All publications up to now have been limited to homogeneous formulations. In this paper, the convolution based method is extended for a heterogeneous formulation of both an immediate and an extended release drug product by including a mixture distribution.

Four different models were evaluated during the model building: The first model used the convolution with the Exponential dissolution model and the logit link function. The average percent error $\%PE$ of both C_{max} and AUC_{last} remained below the 10% criterion as in the guidelines (FIP 1996, CDER 1997), see Table 3. However, the controlled release profiles behave in a bimodal manner, i.e. the profile shows essentially an early, steep peak which originates from the immediate release drug product, followed by a broader peak from the slow release drug product. The early plasma concentrations are systematically underestimated by the traditional model, as can be seen in the parameter AUC_{0-4}. The fact that this model performed adequately based on the criteria stated in the guidelines, even though it underestimates the first four hours, can be explained as follows: as the formulation contained only 25% of immediate release drug product, therefore, the first peak is small and the criterion for C_{max} is primarily fulfilled by the second peak. The part of the observed AUC_{last} corresponding to this initial peak on the other hand represents only a small portion of the total exposure. Therefore, the poor estimation of the initial peak has little effect on the $\%PE$ of the overall AUC_{last}.

The model was therefore extended to the mixture convolution with the logit link function because this used the underlying heterogeneous structure of the capsules and fitted a bimodal profile. The use of this mixture imposes, however, no restriction on the model. It relies on the principle of superposition within pharmacokinetics, i.e., the assumption that each mechanism acts independently of each other and there is linear kinetics. The metabolism of the drug remains unchanged during the drug product release and only depends on the amount of drug product released. The standard convolution model itself assumes already the superposition principle and linear kinetics. The $\%PE$ for C_{max} of this model remains stable, but for AUC_t and AUC_{0-4} the $\%PE$ improved. The fit of the *in-vitro* dissolution data indicated however that further refining was required: the exponential model has a steep incline for the first hours and converges to its asymptotic limit, whereas the *in-vitro* dissolution data showed an asymmetric S-shaped curve. The model was finetuned with the use of the Weibull and the Gompertz model for the *in-vitro* dissolution in combination with the logit link function. However, this does not lead to an additional decrease in $\%PE$. The

lack of improvement in $\%PE$ suggests that small misspecifications in the *in-vitro* dissolution model can not be distinguished from the noise of *in-vivo* testing, such as measurement error, sampling time inaccuracies, ignoring subject dependent absorption due to sparse sampling and other sources of variability. A more intense *in-vivo* sampling scheme shortly after administration of the capsule might have allowed the inclusion of a random effect on the absorption coefficient and as such possibly highlight the difference between the models. Thus, taking into account the heterogeneity of the vessels proves to be more important than small misspecifications in the *in-vitro* dissolution model. Therefore traditional models should not be used in case of formulations consisting of both immediate release and slow release drug product. The risk of overfitting is limited given that the construction of the model is based on the formulation properties and the clearly bimodal profiles.

All models meet the regulatory specifications on the point estimate, see Table 3. Whereas the guidelines (FIP 1996, CDER 1997) focus only on the mean $\%PE$ to be inferior to 10% to conclude IVIVC predictability, this does not take into account the possible variability of the prediction. Even though the average might be inferior to 10%, a large variability of the individual $\%PE$ might indicate that some subject's controlled release profile is poorly estimated. Therefore, one should rather use the non-inferiority philosophy and look at the upper limit of the 90% confidence interval.

A second, more fundamental change to the convolution method of O'Hara (O'Hara *et al.* 2001) is that all models are fitted simultaneously, whereas O'Hara's method first fits the immediate release profile per subject and then fits in a second stage the convolution and the IVIVC using the empirical Bayes estimates of the immediate release PK-profile. A possible drawback of such a two-stage modelling approach is that this might lead to biased results (Verbeke and Molenberghs, 2000). In the first stage, the immediate release PK-profile is reduced to a couple of summary statistics and residual error is ignored. In the second stage, these estimates are used as if they are error-free. Hence, the possible error of these coefficients will be reallocated to the remaining coefficients and as such introduce possibly bias. Fitting everything at once however does not ignore the error in the individual compartmental PK-parameters. On the contrary, it allows a pooling of information about

common parameters of the immediate and the extended release model. This might lead to more accurate parameter estimation like for example the k_a in the case study. However, no formal comparison of the two approaches was performed yet. The advantage of the two-stage approach is that the parameter space is split. As a result, the two-stage approach is more flexible, in the sense of adding random effect, and model convergence is easier and faster.

In conclusion, a novel one-stage methodology was proposed as well as a mixture distribution to cope with heterogeneous formulations in IVIVC testing. Based on the case study it was shown superior to the traditional model.

Acknowledgement

Financial support from the IAP research network nr P5/24 of the Belgian government (Belgian Science Policy) is gratefully acknowledged.

References

BEAL, S.L., and SHEINER, L.B. (1982) Estimating population kinetics. *Critical Reviews in Biomedical Engineering*, **8**, 195 - 222.

CDER (1997) Guidance for industry: Extended release oral dosage forms: development, evaluation, and application of in vitro/in vivo correlations.

COMETS, E., and MENTRE, F. (2001) Evaluation of tests based on individual versus population modelling to compare dissolution curves. *Journal of Biopharmaceutical Statistics*, **11**, 107-123.

DUNNE, A.J., O'HARA, T., and DEVANE, J. (1999) A new approach to modelling the relationship between in vitro and in vivo drug dissolution/absorption. *Statistics in Medicine*, **18**, 1865-1876.

DUNNE, A., GAYNOR, C., and DAVIS, J. (2005) Deconvolution based approach for level A in vivo-in vitro correlation modelling: statistical considerations. *Clinical Research*

and Regulatory Affairs, **22**, 1-14.

FIP (1996) Guidelines for dissolution testing of solid oral products. *Drug Information Journal*, **30**, 1071-1084.

GILLESPIE, W.R., VENG-PEDERSEN, P. (1985) Gastro-intestinal bioavailability: determination of in vivo release profiles of solid dosage forms by deconvolution. *Biopharmaceutics and Drug Disposition*, **6**, 351355.

GILLESPIE, W.R. (1997) Convolution-based approaches for in vivo-in vitro correlation modelling. *Advances in Experimental Mededicine and Biology*, (423), 53-65.

HAYES, S., DUNNE, A., SMART, T., and DAVIS, J. (2004) Interpretation and optimization of the dissolution specifications for a modified release product with an in vivo–in vitro correlation (IVIVC). *Journal of Pharmaceutical Sciences*, **93**, 571-581.

LILIENFELD, S. (2002) Galantamine–a novel cholinergic drug with a unique dual mode of action for the treatment of patients with Alzheimer's disease. *CNS Drug Reviews*, **8**, 159-76.

LINDSEY, J.K. (1997) *Applying generalized linear models*. New York: Springer-Verlag.

MODI, N.B., LAM, A., LINDEMULDER, E., WANG, B., and GUPTA, S.K. (2000) Application of in vitro-in vivo correlations (IVIVC) in setting formulation release specifications. *Biopharmaceutics and Drug Disposition*, 21, 321-326.

MOLENBERGHS, G., and VERBEKE, G. (2005) *Models for Discrete Longitudinal Data.* New York: Springer-Verlag.

O'HARA, T., HAYES, S., DAVIS, J., DEVANE, J., SMART, T., and DUNNE, A. (2001) in vivo–in vitro correlation (IVIVC) modelling incorporating a convolution step. *Journal of Pharmacokinetics and Pharmacodynamics*, **28**, 277-298.

PIOTROVSKY, V., VAN PEER, A., VAN OSSELAER, N., ARMSTRONG, M., and AERSSENS, J. (2003) Galantamine population pharmacokinetics in patients with alzheimer's disease: modelling and simulations. *Journal of Clinical Pharmacology*, **43**, 514-523.

VENG-PEDERSEN, P., GOBBURU, J.V.S., MEYER, M.C., and STRAUGHN, A.B. (2000) Carbamazepine level-A in vivo-in vitro correlation (IVIVC): a scaled convolution based predictive approach. *Biopharmaceutics and Drug Disposition*, **21**, 1-6.

VERBEKE, G., and MOLENBERGHS, G. (2000) *Linear Mixed Models for Longitudinal Data.* New York: Springer-Verlag.

YAFUNE, A., FUNATOGAWA, T., and ISHIGURO, M. (2005) Extended information criterion (EIC) approach for linear mixed effects models under restricted maximum likelihood (REML) estimation. *Statistics in Medicine*, **24**, 3417-3429.

Appendix - SAS Code

As an example, the SAS code for the Gompertz model is given. The odds link function was used. The dataset was structured as follows: capsule numbers were handled as if they were subject levels ("crfid") starting from 1000, whereas the patient numbers remained below 1000. The variable "treat" indicated whether the data was from the immediate or the controlled release formulation. The column "time" stands for the time the sample was taken. Columns "_1" up to "_20" contained the all the sampling times of the *in-vivo* sampling in consecutive order. The plasma concentration or dissolution percentage was in the variable "brval". The variable "indicator" indicates the order of the sample within the subject.

```
proc nlmixed data=ivcp01 method=firo;
    parms lka = 1.5513 lVF = -1.7769 lk21 = -1.5949 lalpha = -2.7590
            lbeta = -1.1698 tlag = 0.1499 s1 = 4.7484 s2 = 0.01 to 0.1
            by 0.01 s2beta = 0.1896 theta0 = 0 theta1 = 0 phi1 = -2.0498
            phi3 = 0.3291 phi4 = 3.5022 phi5 = -1.3546 s0 = 0.02436
            sb4 = 0.2339 sb1 = 0.01 ;

    bounds s0>0;
    array t[20] _1-_20;
    array cp_im[20];
    array cp_ext[20];
    array F2kder[20];
    array expr9[20] ;
    array expr11[20] ;
```

```
array expr13[20] ;
array expr14[20] ;
array expr15[20] ;
array expr18[20] ;
array expr19[20] ;
array expr23[20] ;
array expr31[20] ;

/* In vitro dissolution */
if crfid gt 1000 then do;
    mu = 100*(exp(phi5) + (1-exp(phi1+b1) - exp(phi5))*exp(- exp( phi3 *
        ((phi4+b4) - time)))  );
    sigma = (S0*mu)**2;
    bbeta=0;
end;
/* Immediate release PK profile */
if treat = "IR" and crfid lt 1000 then do;
    ka = exp(lka );
    alpha = exp(lalpha );
    beta = exp(lbeta +bbeta);
    k21 = exp(lk21 );
    VF = exp(lVF);
    common = ka * Dose / VF ;
    A1 = common *(k21 - alpha)/ ((ka-alpha)*(beta-alpha));
    A2 = common *(k21 - beta)/ ((ka-beta)*(alpha-beta));
    A3 = common *(k21 - ka)/ ((alpha-ka)*(beta-ka));
    mu = A1 * exp(-alpha*(time-tlag)) + A2 * exp(-beta*(time-tlag))
        + A3 * exp(-ka*(time-tlag));
    if mu lt 0 then mu = 0;
    sigma=S1**2;
end;

else if treat =: "CR" and crfid lt 1000 then do ;
    t[1] = 0;
    /* Calculation of the convolution */
    if indicator ne 1 then do;
        mu=0;
        do i = 2 to indicator;
            ka = exp(lka );
            alpha = exp(lalpha );
            beta = exp(lbeta +bbeta);
            k21 = exp(lk21 );
            VF = exp(lVF);
            common = ka * Dose / VF ;
            A1 = common *(k21 - alpha)/ ((ka-alpha)*(beta-alpha));
            A2 = common *(k21 - beta)/ ((ka-beta)*(alpha-beta));
            A3 = common *(k21 - ka)/ ((alpha-ka)*(beta-ka));
```

```
            cp_im[i] = A1 * exp(-alpha*(time-tlag - t[i]))
                    + A2 * exp(-beta*(time-tlag - t[i]))
                    + A3 * exp(-ka*(time-tlag - t[i]));

            /* Density function F2' */
            expr3 = exp(phi5);
            expr6 = (1 - (exp(phi1+b1))) - expr3;
            expr9[i] = exp((phi3 * (phi4+b4 - t[i])));
            expr11[i] = exp(( - expr9[i]));
            expr13[i] = expr3 + (expr6 * expr11[i]);
            expr14[i] = 1 - expr13[i];
            expr15[i] = expr13[i]/expr14[i];
            expr18[i] = exp(((theta0 + (theta1 * t[i])) + (log(expr15[i]))));
            expr19[i] = 1 + expr18[i];
            expr23[i] = expr6 * (expr11[i] * (expr9[i] * phi3));
            expr31[i] = expr18[i] * (theta1 + (((expr23[i]/expr14[i]) +
                    ((expr13[i] * expr23[i])/(expr14[i]**2)))/expr15[i]));
            F2kder[i] = (expr31[i]/expr19[i]) - ((expr18[i] * expr31[i])/
                    (expr19[i]**2));

            cp_ext[i] = .5*(cp_im[i] * F2kder[i] + cp_im[i-1] * F2kder[i-1])
                    * (t[i]-t[i-1]);
            mu = mu + cp_ext[i];
            end;
        end;
    ka = exp(lka );
    alpha = exp(lalpha  );
    beta = exp(lbeta +bbeta);
    k21 = exp(lk21 );
    VF = exp(lVF);
    common = ka * Dose / VF ;
    A1 = common *(k21 - alpha)/ ((ka-alpha)*(beta-alpha));
    A2 = common *(k21 - beta)/ ((ka-beta)*(alpha-beta));
    A3 = common *(k21 - ka)/ ((alpha-ka)*(beta-ka));
    cir = A1 * exp(-alpha*(time-tlag)) + A2 * exp(-beta*(time-tlag))
            + A3 * exp(-ka*(time-tlag));

    /* Mixture */
    mu = (exp(phi5))* cir + (1-(exp(phi5))) * mu;
    sigma= ((exp(phi5))*S1)**2 + ((1-(exp(phi5)))*S2)**2  ;

    end;
model brval ~ N(mu, sigma);
random b1 b4 bbeta ~ normal([0, 0, 0],
                            [sb1*sb1,
                                0,   sb4*sb4,
                                0,      0,   s2beta*s2beta]) subject=crfid ;
```

```
predict mu out=empirbayes;
run;
```

Table 1: Parameter estimates (95% confidence interval) for Models 1–4.

	Model 1	Model 2	Model 3	Model 4
	Est.	Est.	Est.	Est.
Parameter	(95% CI)	(95% CI)	(95% CI)	(95% CI)
Immediate Release				
k_a	7.90	8.91	8.65	4.92
	(3.13 ; 19.97)	(4.20 ; 18.92)	(4.11 ; 18.21)	(4.23 ; 5.72)
V_F	0.16	0.17	0.18	0.17
	(0.14 ; 0.19)	(0.16 ; 0.18)	(0.17 ; 0.19)	(0.16 ; 0.18)
k_{21}	0.39	0.17	0.13	0.20
	(0.13 ; 1.20)	(0.10 ; 0.29)	(0.06 ; 0.29)	(0.14 ; 0.30)
α	0.08	0.07	0.08	0.06
	(0.06 ; 0.10)	(0.06 ; 0.09)	(0.05 ; 0.12)	(0.05 ; 0.07)
β	0.56	0.26	0.20	0.32
	(0.18 ; 1.68)	(0.18 ; 0.39)	(0.13 ; 0.31)	(0.22 ; 0.45)
t_{lag}	0.29	0.33	0.33	0.23
	(0.09 ; 0.49)	(0.20 ; 0.46)	(0.20 ; 0.46)	(0.20 ; 0.26)
σ_δ	5.06	5.03	5.08	5.18
	(4.61 ; 5.50)	(4.61 ; 5.46)	(4.64 ; 5.52)	(4.73 ; 5.63)
σ_β	0.16	0.20	0.20	0.17
	(0.09 ; 0.23)	(1.13 ; 1.31)	(0.12 ; 0.29)	(0.11 ; 0.24)
In Vitro Dissolution				
ϕ_1	1.00	1.00	0.90	0.88
	(0.97 ; 1.03)	(0.97 ; 1.03)	(0.88 ; 0.92)	(0.85 ; 0.90)
ϕ_2	0.12	0.12	1.45	3.24
	(0.11 ; 0.14)	(0.11 ; 0.14)	(1.38 ; 1.52)	(2.86 ; 3.61)

Table 1: Parameter estimates (95% confidence interval) for Models 1–4. (continued)

	Model 1	Model 2	Model 3	Model 4
	Est.	Est.	Est.	Est.
Parameter	(95% CI)	(95% CI)	(95% CI)	(95% CI)
ϕ_3	-1.56	0.18	7.88	0.33
	(-1.80 ; -1.32)	(-0.33 ; 0.39)	(7.49 ; 8.27)	(0.31 ; 0.35)
ϕ_5		0.20	0.24	0.27
		(0.19 ; 0.22)	(0.23 ; 0.25)	(0.26 ; 0.29)
σ_1	3.00	2.94	1.94	0.02
	(2.57 ; 3.43)	(2.52 ; 3.35)	(1.65 ; 2.22)	(0.02 ; 0.03)
σ_{ϕ_2}	0.09	0.16	1.23	1.19
	(0.04 ; 0.13)	(0.09 ; 0.23)	(0.71 ; 1.75)	(0.67 ; 1.73)
σ_{ϕ_1}				0.25
				(0.13 ; 0.37)
Mixture Convolution				
θ_0	0.55	-0.37	0.32	-0.45
	(0.34 ; 0.76)	(-0.63 ; -0.11)	(0.09 ; 0.55)	(-0.80 ; -0.11)
θ_1	0.16	0.06	-0.07	0.18
	(0.11 ; 0.22)	(0.03 ; 0.10)	(-0.10 ; -0.04)	(0.13 ; 0.23)
σ_2	3.38	1.04	0.73	1.22
	(3.08 ; 3.69)	(0.83 ; 1.25)	(0.35 ; 1.12)	(0.70 ; 1.74)

Table 2: Parameter estimates of the Gompertz Odds Model Compared to the Population Modelling (Piotrovsky 2003) applied on several studies on elderly patients.

	Gompertz Odds	Population Model
k_a	4.29	3.05
V_f	0.17	0.18
k_{21}	0.20	0.07
α	0.06	0.04
β	0.32	0.10

Table 3: Average Absolute Percent Prediction Error and its 90% confidence interval.

Model	C_{max}		AUC_t		AUC_{0-4}	
1	5.12	(3.17 ; 8.25)	6.54	(3.55 ; 12.05)	15.27	(11.56 ; 20.18)
2	5.28	(3.22 ; 8.66)	2.87	(1.02 ; 8.10)	6.68	(4.07 ; 11.06)
3	8.16	(6.52 ; 10.21)	4.13	(2.22 ; 7.66)	7.88	(5.33 ; 11.66)
4	3.76	(2.39 ; 5.93)	6.49	(4.27 ; 9.86)	6.25	(4.52 ; 8.63)

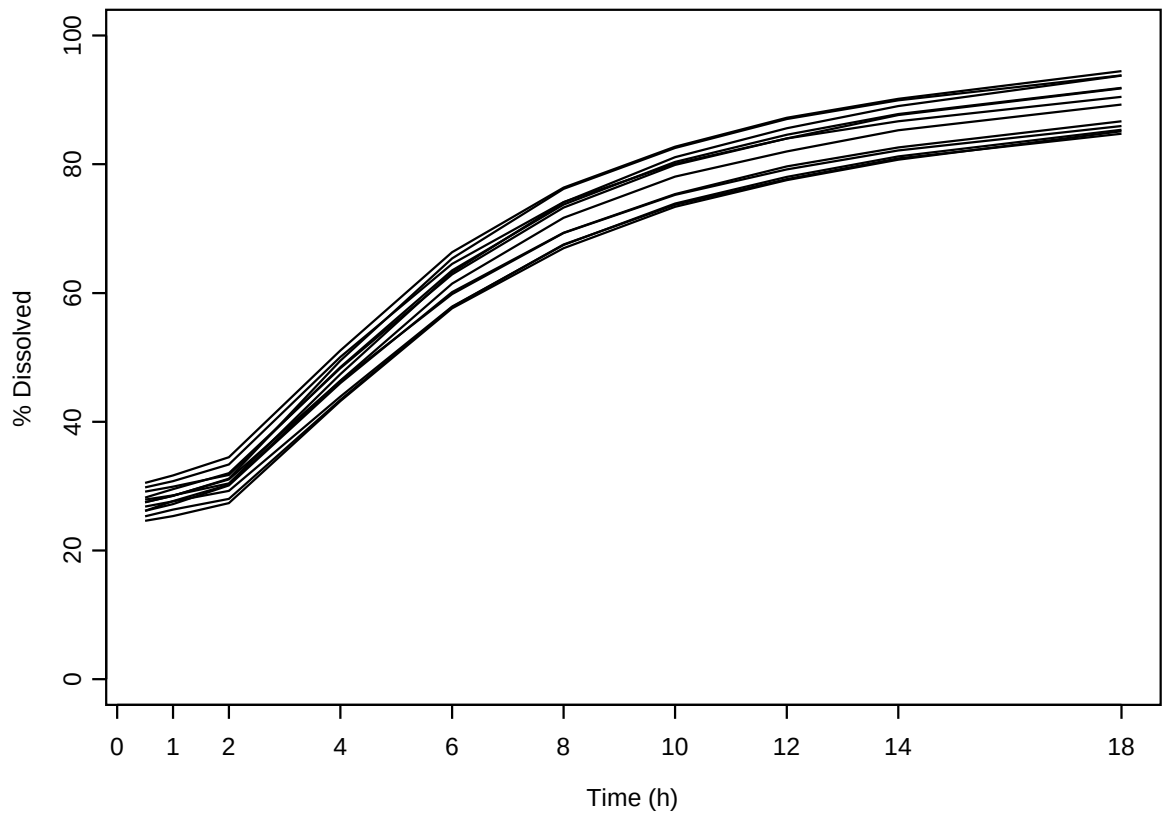

Figure 1: *In-Vitro* Dissolution Curves of Individual Capsules of the Controlled Release Formulation

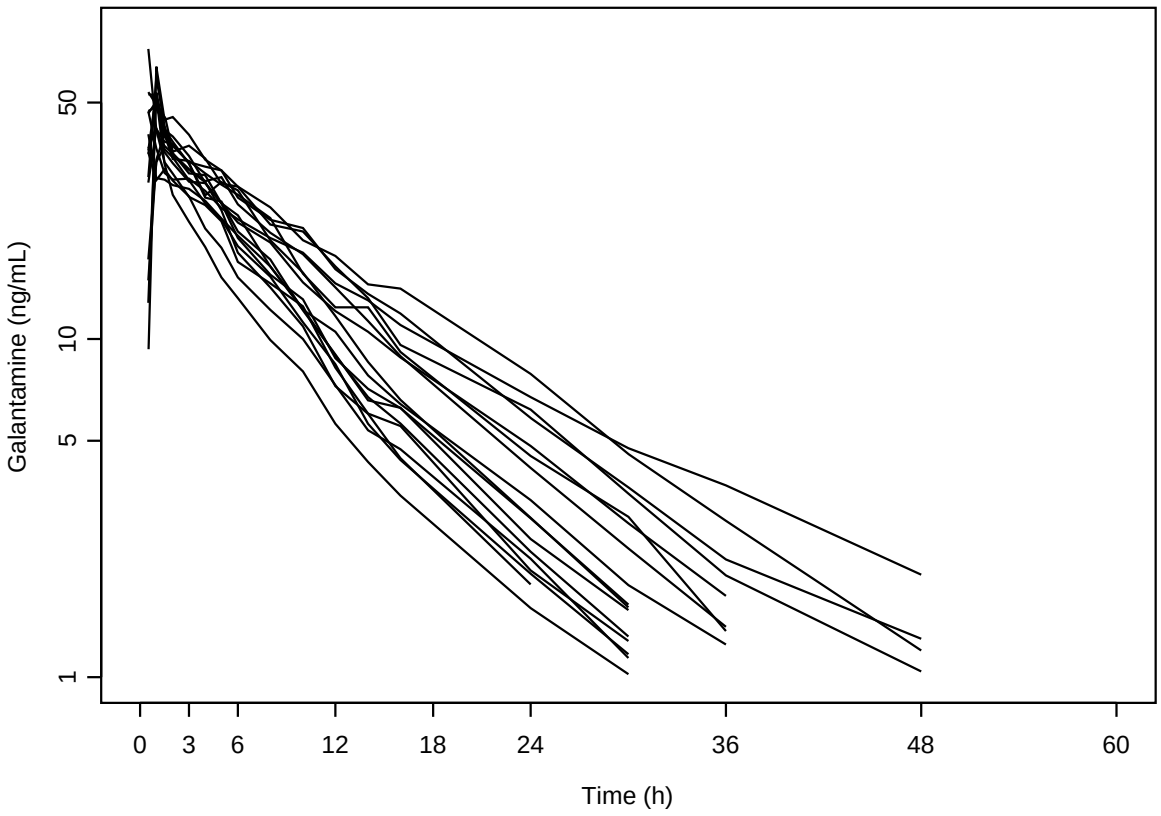

Figure 2: Individual *In-Vivo* Plasma Concentrations for the Immediate Release Formulation of Galantamine.

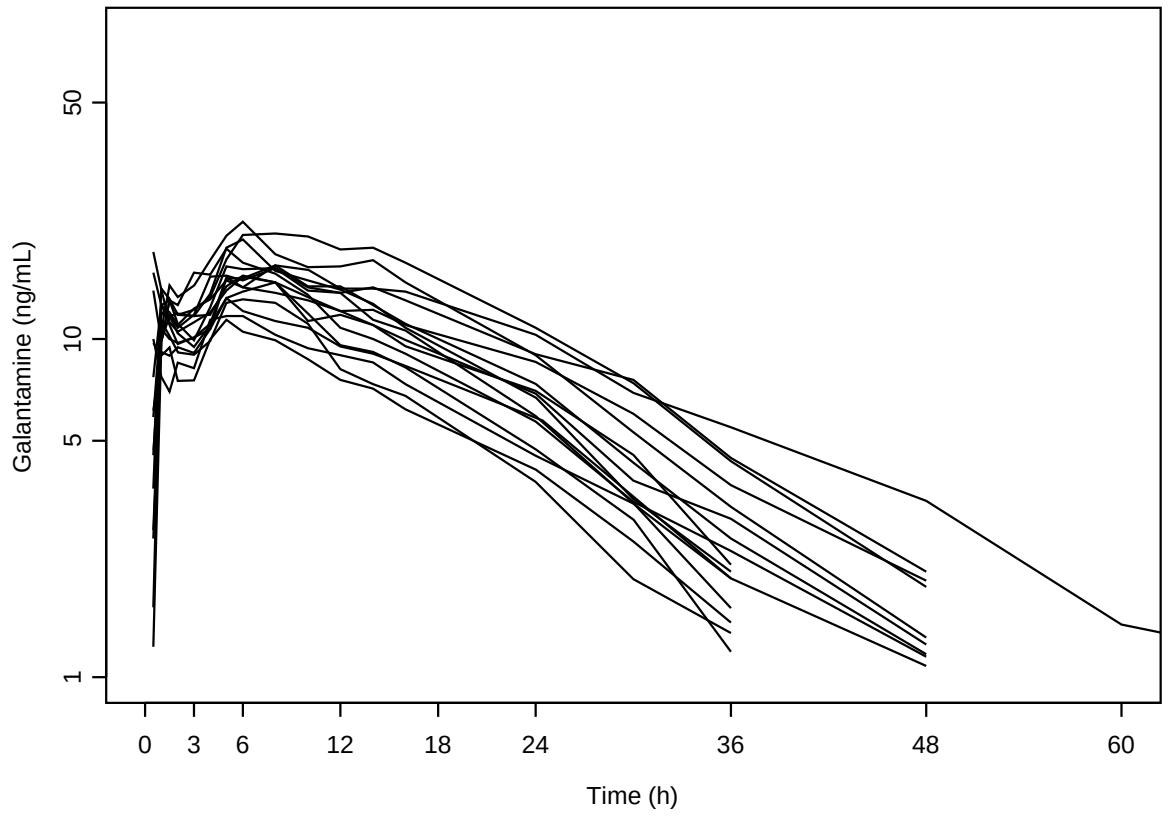

Figure 3: Individual *In-Vivo* Plasma Concentrations for the Controlled Release Formulation of Galantamine.

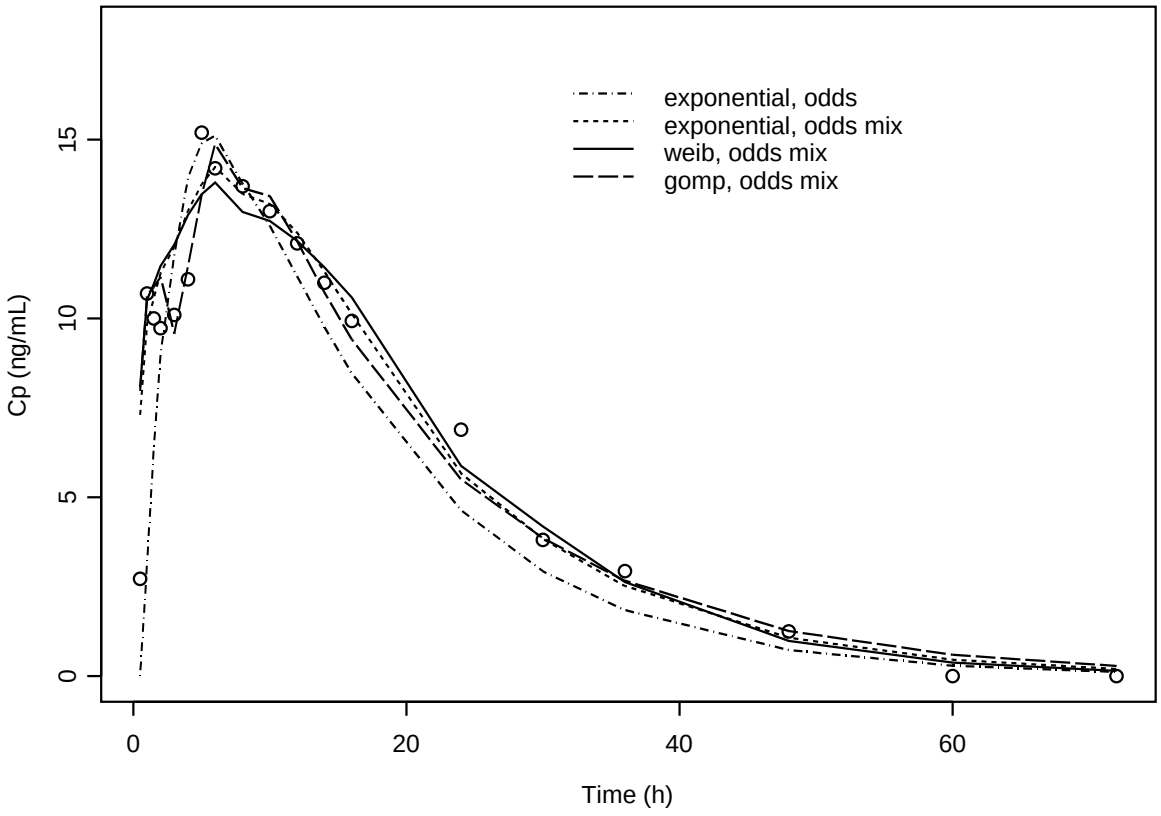

Figure 4: Observed and Predicted Controlled Release Galantamine Concentrations of one Subject for the Different Models.

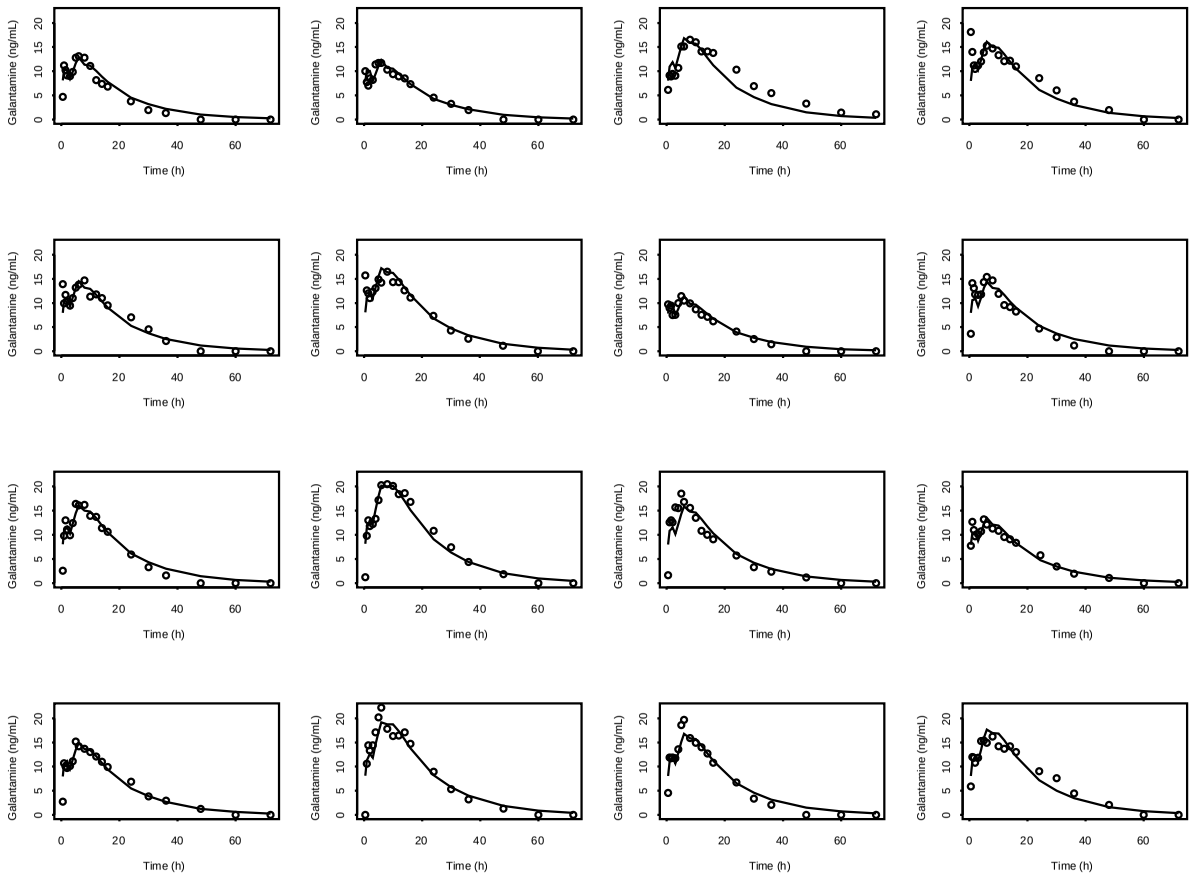

Figure 5: Observed and Predicted Controlled Release Galantamine Concentrations per Subject for the Gompertz Odds Model.

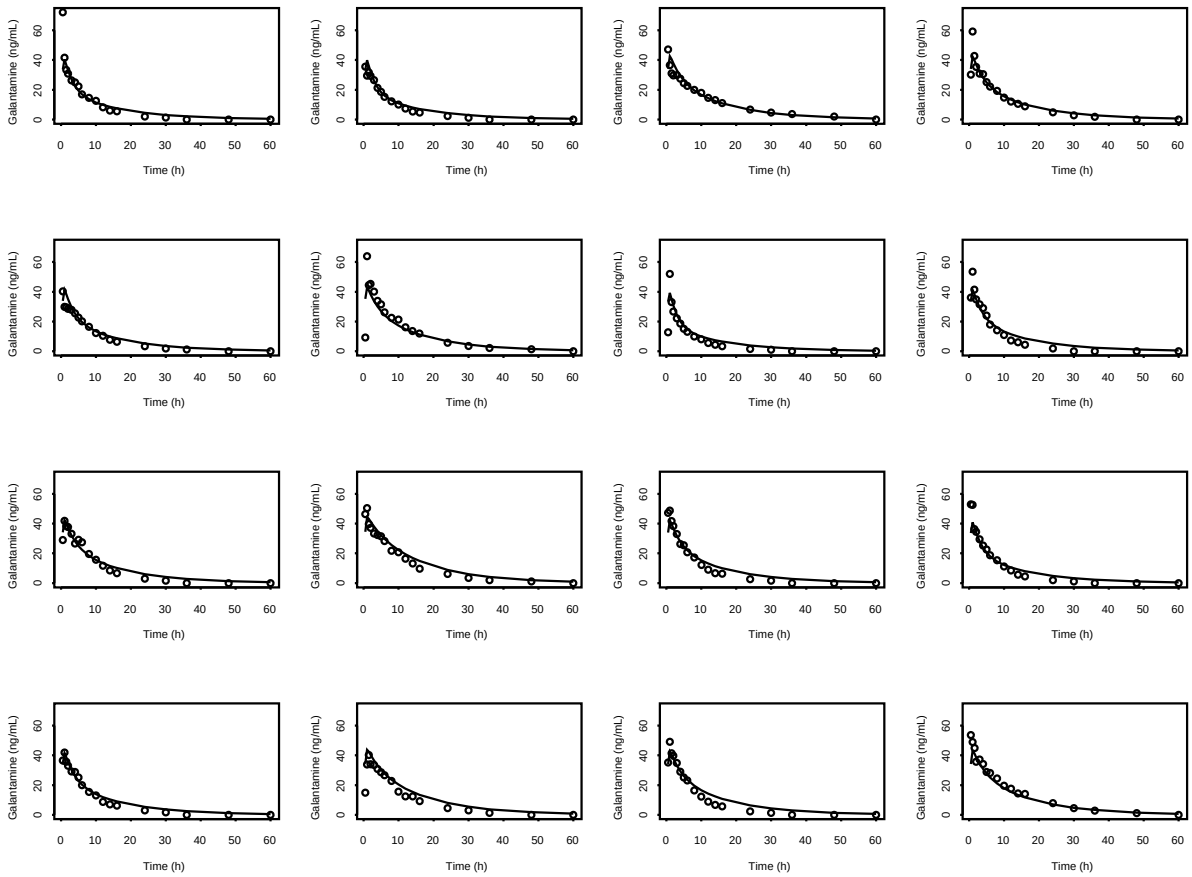

Figure 6: Observed and Predicted Immediate Release Galantamine Concentrations per Subject for the Gompertz Odds Model.

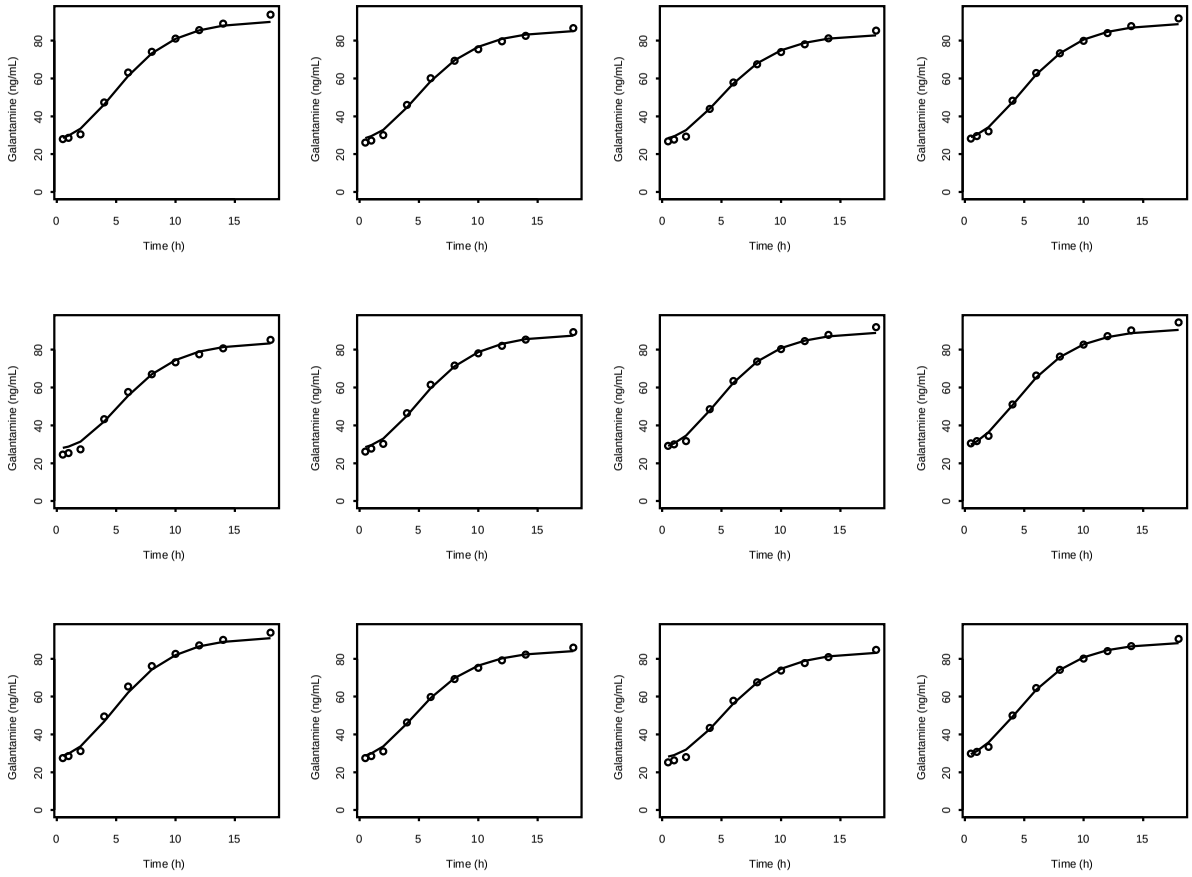

Figure 7: Observed and Predicted In-Vitro Dissolution per Capsule for the Gompertz Odds Model.

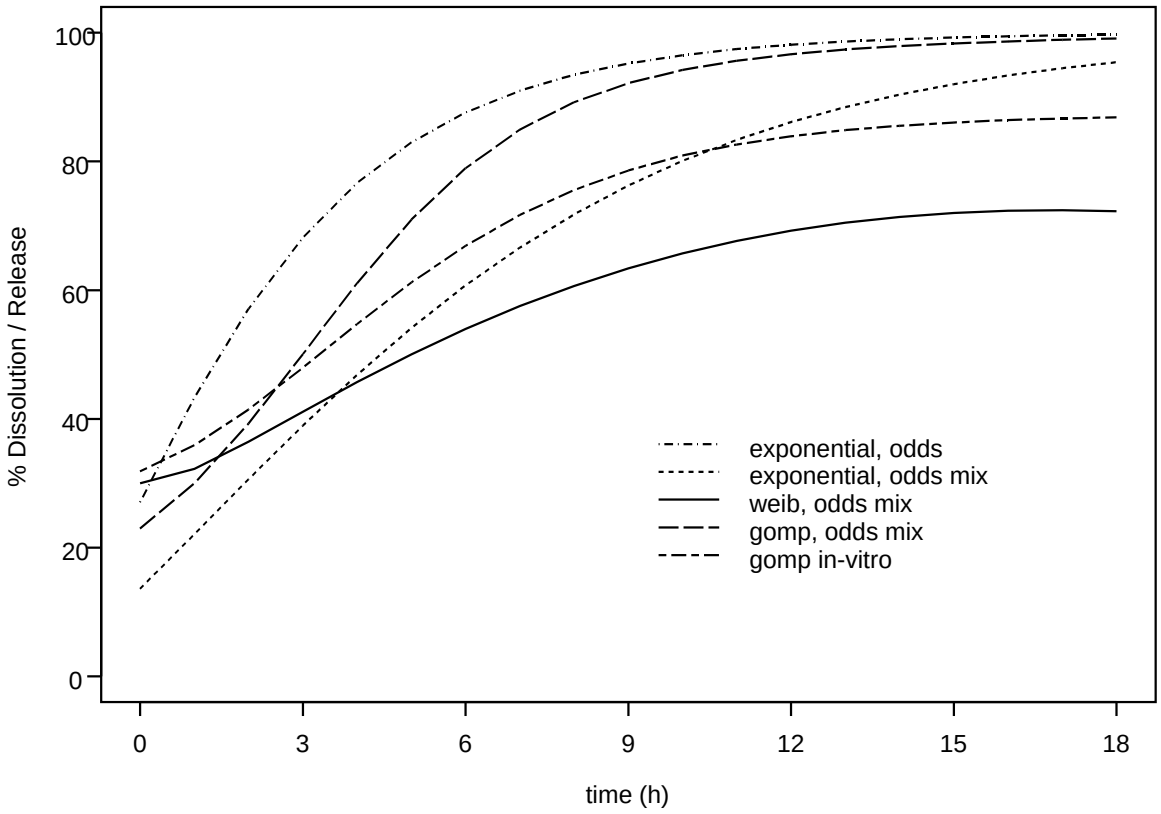

Figure 8: Marginalized *In-Vivo* Release Prediction.

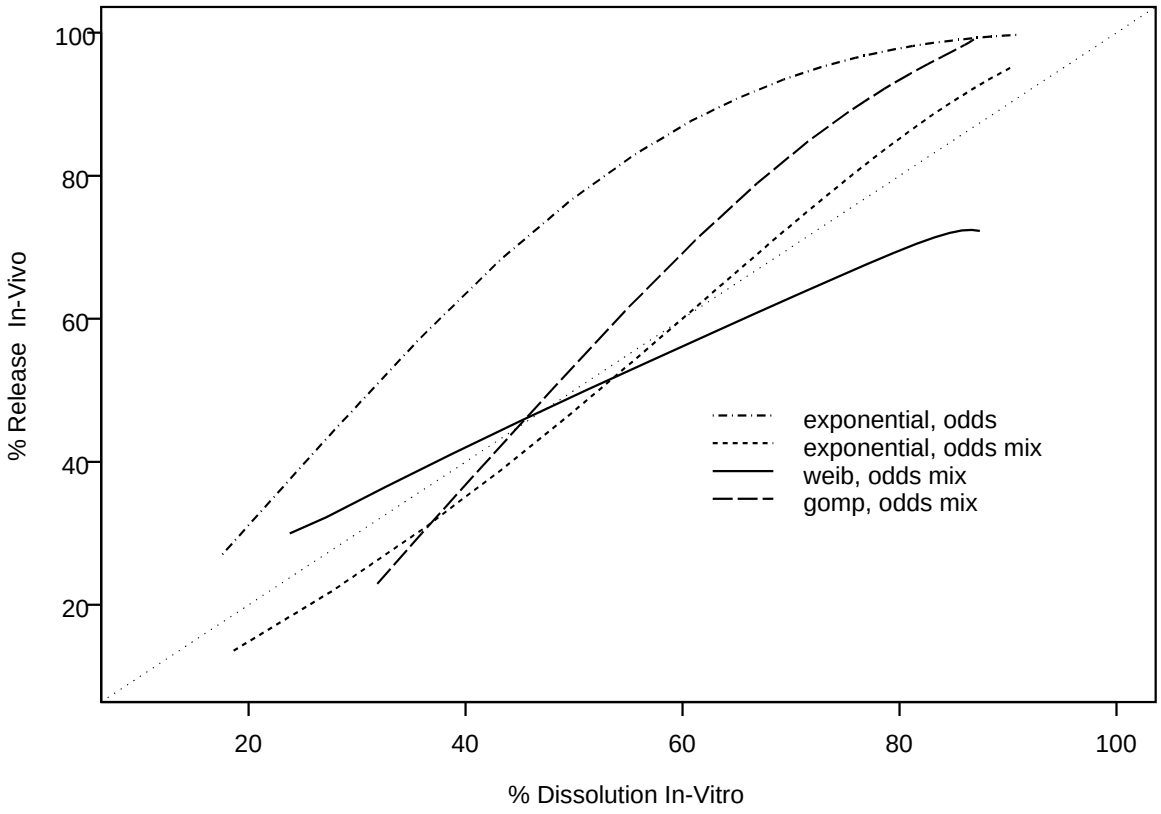

Figure 9: Marginalized *In-Vitro* Dissolution versus *In-Vivo* Release Prediction.